Time-resolved photoluminescence from ZnO nanostructures

W. M. Kwok
Department of Chemistry, The University of Hong Kong, Pokfulam Road, Hong Kong

A. B. Djurišić[a] and Y. H. Leung
Department of Physics, The University of Hong Kong, Pokfulam Road, Hong Kong

W. K. Chan and D. L. Phillips
Department of Chemistry, The University of Hong Kong, Pokfulam Road, Hong Kong

(Received 28 June 2005; accepted 4 October 2005; published online 22 November 2005)

Different ZnO nanostructures (tetrapods, shells, rods, and highly faceted rods) were characterized by photoluminescence (PL) and time-resolved PL measurements. It was found that different nanostructures exhibit very different optical properties in terms of defect emission and decay times of the spontaneous emission. No correlation was found between the PL decay times and defect emission intensities and defect emission positions. The short decay times of the UV emission are most likely due to nonradiative defects that are correlated with the crystalline quality and do not contribute to the visible emission. Neither short PL decay times nor intense defect emissions rule out achievement of stimulated emission. © *2005 American Institute of Physics*.
[DOI: 10.1063/1.2137456]

The optical properties of ZnO have been extensively studied.[1–19] Time-resolved photoluminescence (TRPL) studies have been reported for spontaneous[1,7–14] and stimulated emission[1–6] in ZnO. However, there is large dispersion of the results from different studies. For example, Özgür *et al.*[1] reported that spontaneous recombination in ZnO films can be described with a single exponential decay curve with time constants in the 30–74 ps range, depending on the annealing temperature of the film. Koida *et al.*[10,11] also reported exponential decay for epitaxial films, with decay times ranging from 46 to 110 ps. On the other hand, biexponential decays were reported for ZnO single crystal,[10,11] nanowires,[2] nanorods,[12,19] and thin films.[8,9] Different decay constants for thin films were reported, ranging from $\tau_1=30-50$ ps and $\tau_2=100-400$ ps (Ref. 8) to $\tau_1=180$ ps and $\tau_2=1.0$ ns.[9] The initial fast decay was attributed to the capture of excitons and carrier trapping by deep levels, followed by nonradiative relaxation processes.[8] It was also proposed that the fast decay is due to the free exciton decay, while the slow decay is due to bound excitons. However, bound exciton emission diminishes above 160 K,[14] so that this assignment of decay processes at room temperature is unlikely. It was recently reported that two decay constants (100 and 700 ps) are due to different decay times of nonlinear *M* band and free exciton emission.[7]

We studied photoluminescence from different ZnO nanostructures: tetrapod nanowires, shells, rods, and highly faceted rods. The nanostructures studied exhibited different defect emission positions and different UV to visible emission ratios, and thus enable us to examine the influence of defect emission intensity and position on the photoluminescence dynamics and achievement of stimulated emission. The relationship between the decay time constants of the UV emission, UV to visible emission intensity, sample morphology and crystallinity, and achievement of stimulated emission was investigated. It should be noted that the measurements were performed on an ensemble of the nanostructures, so that nanostructures of different sizes contribute to the measured luminescence. For the size ranges investigated, no quantum size effects are expected, but there can be some variation in the observed decay constants and defect emission due to different surface to volume ratios of nanostructures with different sizes. However, these differences are less significant in the samples which are sufficiently large.

The tetrapod nanowires,[5] rods,[15] hollow shells,[16] and highly faceted rods[20] were prepared according to previously reported procedures. The morphology of the nanostructures obtained was examined by scanning electron microscopy (SEM) using a Leo 1530 field emission SEM and transmission electron microscopy (TEM) and selected area electron diffraction using Philips Tecnai-20 TEM and JEOL 2010F TEM. Wide range cw photoluminescence (PL) was measured using a HeCd laser excitation source (325 nm). TRPL and integrated photoluminescence PL were measured by using the Kerr gated fluorescence technique, which has been described in detail elsewhere.[21]

Figure 1 shows SEM and TEM images of the studied nanostructures. Tetrapods typically have a leg diameter in the range 100–200 nm, which tapers off into a nanowire with a diameter of 20–40 nm. The total leg length is in the 1–4 μm range. The shells have a diameter in the 300 nm–2 μm range, while the rods synthesized by the hydrothermal method have diameters in the 30–50 nm range. The highly faceted rods have the largest diameters, in the 200 nm–1 μm range. The density of the nanostructures with a laser spot size ($\sim$100 μm diameter) was less than 10 for the tetrapods, $\sim$100 for the shells, several thousand for the rods, and $\sim$20 for the faceted rods. It can be observed that ZnO hollow shells consist of a large number of small crystallites. The ZnO rods synthesized by a hydrothermal method exhibit less clear crystal facets and inferior crystal quality compared to ZnO tetrapods and highly faceted rods. Figure 2 shows the PL spectra and PL decay curves of the different nanostructures. Figure 2(a) shows the integrated PL spectra in the UV spectral range. It can be observed that the position of the UV peak is different for different nanostructures.

[a]Electronic mail: dalek@hkusua.hku.hk

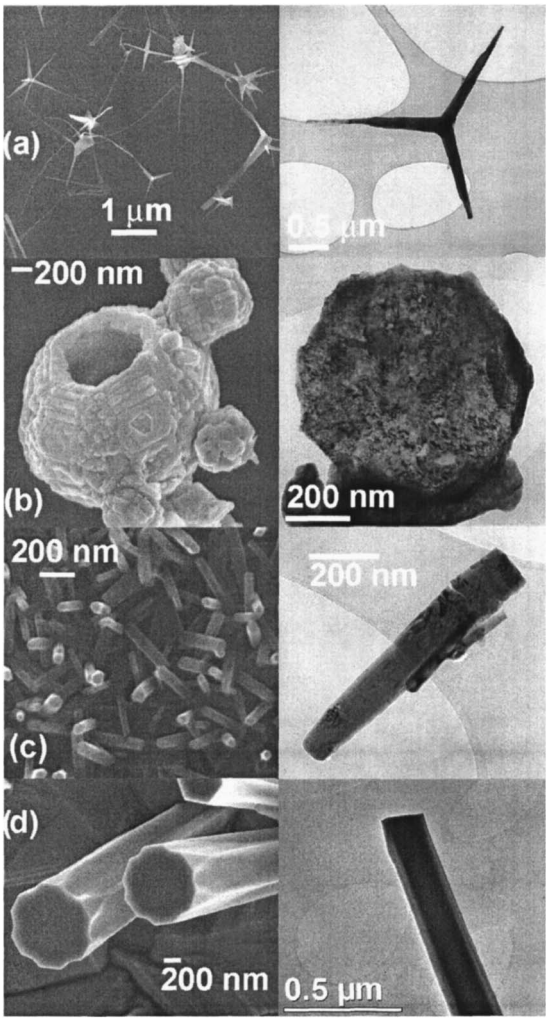

FIG. 1. Representative SEM (left) and TEM (right) images of ZnO (a) tetrapods, (b) shells, (c) rods, and (d) highly faceted rods.

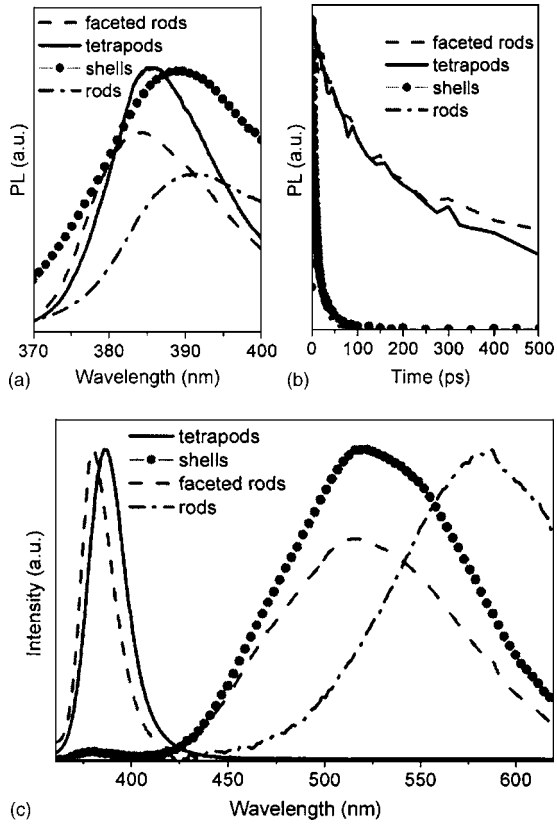

FIG. 2. (a) Integrated photoluminescence spectra from different ZnO nanostructures. (b) Photoluminescence decay curves. (c) Wide range photoluminescence from different ZnO nanostructures.

While there can be small (1–2 nm) variations in the peak position in the spectra excited from different areas of the sample, the UV emission from rods and shells is in general redshifted compared to the tetrapods and faceted rods. TRPL measurements reveal that all the investigated structures exhibit biexponential decay, in agreement with other reports in the literature.[8–12,19] However, as clearly observed from Fig. 2(b), the decay time constants are very different. The tetrapods exhibit comparatively slow decay with time constants of 91 and 708 ps. The shells exhibit considerably faster decay, with time constants of 10 and 37 ps. The rods also show fast decay, with time constants of 7 and 44 ps. The faceted rods, on the other hand, show slow decay with time constants of 111 ps and 1.1 ns. These time constants are comparable to those of high quality ZnO epitaxial layers (180 ps and 1.0 ns).[9] Therefore, we can observe that the largest structures (tetrapod nanowires and highly faceted rods) exhibit the slowest decay.

It was reported that the decay times of ZnO nanorods are size dependent, and that decay constants increase as the size increases.[12] It was proposed that the linear size dependence of the longer decay constant is radiative in origin, and that it can be explained by exciton-polariton effects.[12] The minimum radiative lifetime predicted by the exciton-polariton model was ~260 ps (Ref. 12) (for a nanosphere with 17 nm radius).[12] However, this minimum lifetime is much longer than that obtained for the rods and hollow shells (44 and 37 ps), which indicates that the exciton-polariton model is not applicable in these structures. For ZnO thin films, it was found that the bound exciton decay time is dependent on the grain size, and it varied from 47 ps for 40 nm grains to 216 nm for 200 nm grains.[13] It should be noted that the bound excitons have faster decay times which is likely due to efficient capture processes leading to bound excitons at low temperatures.[14] Therefore, it is likely that there is some relationship between the grain or nanostructure size and the PL decay time constants, although no simple size dependence can be derived for nanostructures with different morphologies prepared by different fabrication methods.

However, different fabrication methods enable us to obtain not only different sizes and morphologies but also different positions and intensities of defect emissions, so that we could examine possible connections between the visible defect emissions and the UV PL decay times. The wide range of PL spectra obtained for different nanostructures, showing different intensities and positions of defect emissions, are given in Fig. 2(c). Green and yellow defect luminescence were found to have different origins, green luminescence was due to the defects located at the surface, while yellow luminescence was due the defects in the bulk of the nanorods.[15] However, the fast PL decay times have been observed in samples with both yellow (rods) and green (shells) emissions. Since the samples exhibiting prominent green emission can have very fast (shells) or very slow (highly faceted rods) decays, obviously there is no clear relationship between the UV to green defect emission ratios and the photoluminescence decay times in different nanostructures. This

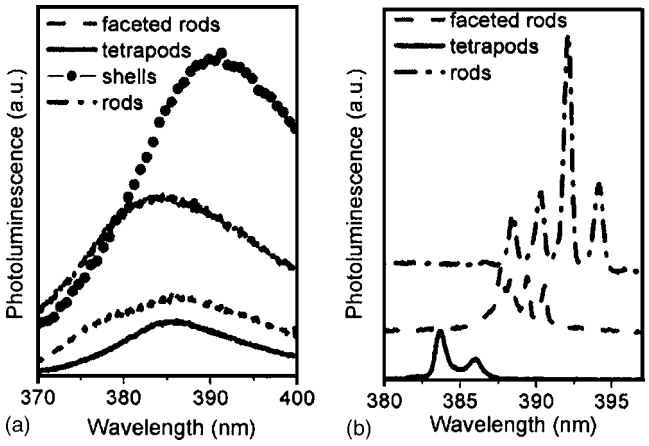

FIG. 3. Time-resolved photoluminescence spectra at 5 ps at (a) low pump fluence and (b) high pump fluence.

is also supported by the fact that reported results on ZnO nanorod arrays which show no visible PL have faster decay constants (~80 and ~360 ps) than the highly faceted rods which have comparable intensities of UV and green emission.[19]

It was proposed that the nonradiative defects in ZnO which determine the PL decay time are defect species containing zinc vacancy, such as vacancy complexes.[10,11] It was also shown that both fast and slow decay constants can be increased by annealing the samples in a forming gas,[14] indicating the importance of the native defects in the carrier relaxation processes. However, the lack of correlation between the green emission intensity and the PL decay time constants for both the fast and slow processes of the biexponential decay indicate that different defects or defect complexes are involved in the processes responsible for the defect luminescence and carrier trapping followed by nonradiative relaxation. The hypothesis that the short decay times are due to nonradiative recombination centers is in agreement with a previous report on emission from ZnO thin films.[1]

Figure 3 shows the time-resolved spectra at 5 ps for spontaneous and stimulated emission for different nanostructures. All the nanostructures except the hollow shells exhibit stimulated emission, as shown in Fig. 3(b). The lasing thresholds obtained are 45 $\mu J/cm^2$ for faceted rods, ~102 $\mu J/cm^2$ for tetrapod nanowires,[5] and ~480 $\mu J/cm^2$ for rods. It should be noted that a direct comparison of the lasing thresholds among different works in the literature is difficult, due to differences in the fabrication methods and the dimensions of the nanostructures and differences among individual nanostructures. However, it is still possible to compare the data on defect emission, spontaneous emission decay constants, and observation of stimulated emission. We found that the stimulated emission is still possible in ZnO rods, in spite of the fast recombination time. The connection between the slow decay time constants, the crystalline quality of the samples, and the observation of stimulated emission is commonly implied in the literature. Previously reported time constants for biexponential decay in ZnO nanowires were $\tau_1=70$ ps and $\tau_2=350$ ps.[2] These wires exhibited lasing with a threshold of 40 kW/cm^2 (or 120 $\mu J/cm^2$).[2] Similar results were obtained for ZnO nanorod arrays and the time constants obtained for spontaneous emission were ~80 and ~360 ps, while the lasing threshold was 130 $\mu J/cm^2$.[19] However, Özgür *et al.*[1] reported stimulated emission (at an excitation density of ~50 $\mu J/cm^2$) from ZnO thin films which showed fast recombination times $\leqslant$74 ps, which is in agreement with the results obtained in our work. Therefore, while there is a connection between the crystalline quality of the sample and the decay time constants of the spontaneous emission, slow spontaneous emission decay is not a necessary condition for the achievement of the stimulated emission.

To summarize, we have performed time-resolved and time-integrated photoluminescence measurements on different ZnO nanostructures. We found that there is no obvious relationship between the position of the defect luminescence, the ratio of UV to visible emission, and the decay constants of the spontaneous emission. We also found that the fast decay of the spontaneous emission does not imply that stimulated emission cannot be achieved.

This work is partly supported by the Research Grant Council of the Hong Kong Special Administrative Region, China (Project Nos. HKU 1/01C and HKU 7021/03P to D.L.P. and HKU 7019/04P to A.B.D.).

[1] Ü. Özgür, A. Teke, C. Liu, S.-J. Cho, H. Morkoç, and H. O. Everitt, Appl. Phys. Lett. **84**, 3223 (2004).
[2] M. H. Huang, S. Mao, H. Feick, H. Yan, Y. Wu, H. Kind, E. Weber, R. Russo, and P. Yang, Science **292**, 1897 (2001).
[3] J. C. Johnson, K. P. Knutsen, H. Yan, M. Law, Y. Zhang, P. Yang, and R. J. Saykally, Nano Lett. **4**, 197 (2004).
[4] J. C. Johnson, H. Yan, P. Yang, and R. J. Saykally, J. Phys. Chem. B **107**, 8816 (2003).
[5] Y. H. Leung, W. M. Kwok, A. B. Djurišić, D. L. Phillips, and W. K. Chan, Nanotechnology **16**, 579 (2005).
[6] J. M. Sarko, J. K. Song, C. W. Blackledge, I. Swart, S. R. Leone, S. Li, and Y. Zhao, Chem. Phys. Lett. **404**, 171 (2005).
[7] H. Priller, R. Hauschild, J. Zeller, C. Klingshirn, H. Kalt, R. Kling, F. Reuss, Ch. Kirchner, and A. Waag, J. Lumin. **112**, 173 (2005).
[8] B. Guo, Z. Ye, and K. S. Wong, J. Cryst. Growth **253**, 252 (2003).
[9] S. W. Jung, W. I. Park, H. D. Cheong, G.-C. Yi, H. M. Jang, S. Hong, and T. Joo, Appl. Phys. Lett. **80**, 1924 (2002).
[10] T. Koida, S. F. Chichibu, A. Uedono, A. Tsukazaki, M. Kawasaki, T. Sota, and H. Koinuma, Appl. Phys. Lett. **82**, 532 (2003).
[11] T. Koida, A. Uedono, A. Tsukazaki, T. Sota, M. Kawasaki, and S. F. Chichibu, Phys. Status Solidi A **201**, 2841 (2004).
[12] S. Hong, T. Joo, W. I. Park, Y. H. Jun, and G.-C. Yi, Appl. Phys. Lett. **83**, 4157 (2003).
[13] T. Matsumoto, H. Kato, K. Miyamoto, M. Sano, and E. Z. Zhukov, Appl. Phys. Lett. **81**, 1231 (2002).
[14] A. Teke, Ü. Özgür, S. Doğan, X. Gu, H. Morkoç, B. Nemeth, J. Nause, and H. O. Everitt, Phys. Rev. B **70**, 195207 (2004).
[15] D. Li, Y. H. Leung, A. B. Djurišić, Z. T. Liu, M. H. Xie, S. L. Shi, S. J. Xu, and W. K. Chan, Appl. Phys. Lett. **85**, 1601 (2004).
[16] Y. H. Leung, K. H. Tam, A. B. Djurišić, M. H. Xie, W. K. Chan, Ding Lu, and W. K. Ge, J. Cryst. Growth **283**, 134 (2005).
[17] B. K. Meyer, H. Alves, D. M. Hofmann, W. Kreigseis, D. Forster, F. Bertram, J. Christen, A. Hoffmann, M. Straßburg, M. Dworzak, U. Haboeck, and A. V. Rodina, Phys. Status Solidi B **241**, 231 (2004).
[18] A. B. Djurišić, W. C. H. Choy, V. A. L. Roy, Y. H. Leung, C. Y. Kwong, K. W. Cheah, T. K. Gundu Rao, W. K. Chan, H. F. Lui, and C. Surya, Adv. Funct. Mater. **14**, 856 (2004).
[19] X. Han, G. Wang, Q. Wang, L. Cao, R. Liku, B. Zou, and J. G. Hou, Appl. Phys. Lett. **86**, 223106 (2005).
[20] Y. H. Leung, A. B. Djurišić, and M. H. Xie, J. Cryst. Growth **284**, 80 (2005).
[21] C. Ma, W. M. Kwok, W. S. Chan, P. Zuo, J. T. W. Kan, P. H. Toy, and D. L. Phillips, J. Am. Chem. Soc. **127**, 1463 (2005).